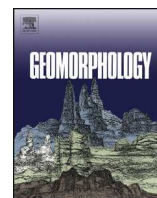




Contents lists available at ScienceDirect

Geomorphology

journal homepage: www.elsevier.com/locate/geomorph

Sedimentological and geomorphological imprints of Holocene tsunamis in southwestern Spain: An approach to establish the recurrence period

Francisco Ruiz ^{a,*}, Joaquín Rodríguez-Vidal ^a, Manuel Abad ^a, Luis M. Cáceres ^a, María I. Carretero ^b, Manuel Pozo ^c, José M. Rodríguez-Llanes ^d, Francisco Gómez-Toscano ^e, Tatiana Izquierdo ^f, Eric Font ^g, Antonio Toscano ^a

^a Departamento de Geodinámica y Paleontología, Campus del Carmen, Universidad de Huelva, 21071 Huelva, Spain

^b Departamento de Cristalografía, Mineralogía y Química Agrícola, Universidad de Sevilla, 41071 Sevilla, Spain

^c Departamento de Geología y Geoquímica, Universidad Autónoma de Madrid, Madrid, Spain

^d Centre for Research on the Epidemiology of Disasters, Institute of Health and Society, Université catholique de Louvain, 1200 Brussels, Belgium

^e Departamento de Historia I, Campus del Carmen, Universidad de Huelva, 21071 Huelva, Spain

^f Centro de Vulcanología e Avaliação de Riscos Geológicos, Universidade dos Açores, 9500-321 Ponta Delgada, Portugal

^g IDL-FCUL, Faculdade de Ciências de Lisboa, Campo Grande, 1749-016 Lisboa, Portugal

ARTICLE INFO

Article history:

Received 2 March 2012

Received in revised form 29 August 2013

Accepted 10 September 2013

Available online xxxx

Keywords:

Geomorphology

Tsunami

Recurrence

Holocene

SW Spain

ABSTRACT

This paper reviews the sedimentological and geomorphological imprints of prehistoric and historical tsunamis in the four main estuaries of SW Spain. These imprints include beach erosion, filling of intertidal channels, deposition of bioclastic layers, washover fans and reworked aeolian sheets and the breaching of spits and tombolos. Most of these imprints were caused by the 218–209 BC and AD 1755 tsunamis, although evidence of other tsunamis has been identified. In these two events, effects on human populations were severe and diverse, such as human loss of life, changes in coastal settlements and international borders, damage to port infrastructure or flooding of marsh and inhabited areas. New radiocarbon reservoir data were included in order to obtain an approach to the recurrence period of these high-energy events (700–1000 years) in this area.

© 2013 Elsevier B.V. All rights reserved.

1. Introduction

In recent years, numerous investigations have focused on the geomorphic evidence of the 2004 Indian Ocean tsunami along the coasts of Indonesia, Thailand and Sri Lanka. These imprints include the formation of new inlets and the breaching of barrier islands (Mascarenhas, 2006), extensive erosion in river mouths and tidal channels (Szczucinski et al., 2006), return channels (Fagherazzi and Du, 2008) or area reduction in reef islands (Kench et al., 2008). In this sense, the post-tsunami effects have been extensively analysed through the comparison of pre- and post-tsunami data and satellite imagery in order to calculate coastal recovery (Choowong et al., 2009; Liew et al., 2010) or bathymetric changes in the nearshore zone (Goto et al., 2011). The general conclusion is that this event caused strong geomorphic changes (Paris et al., 2009), which has played a determinant role in the subsequent development of these areas (e.g. Siwar et al., 2006).

Lessons from this tsunami have been applied to the geological record and have resulted in interesting findings. Multi-proxy analyses of sediment cores helped to identify palaeotsunamis, with the recognition of tsunamigenic facies and their sedimentological, mineralogical,

geochemical and micropalaeontological features (Monecke et al., 2008; Goff et al., 2010).

In this paper, we summarize the main sedimentological and geomorphological imprints of Holocene tsunamis in the main four estuaries of southwestern Spain and their implications for human settlements and activities during historical times. In addition, a new approach to estimate the recurrence period of these high-energy events is proposed.

2. Study area

2.1. General features

In the southwestern Spanish coast (Fig. 1), four main estuaries may be differentiated on a clastic Plio–Pleistocene substrate: (1) the Guadiana Estuary, composed of a main channel (5–15 m depth) and broad marsh deposits protected by sandy spits and separated by distributary channels near the mouth (Fig. 2A); (2) the Tinto–Odiel Estuary (Fig. 3A), with a marine sector constituted by two main channels that separate salt-marsh deposits; (3) the Guadalquivir Estuary (Fig. 4A), partially closed by two spits (Doñana and La Algaída) that protect the Doñana National Park, a biosphere reserve (>50,000 ha) with a sedimentary record from the Lower Pliocene to the Late Holocene (Salvany et al., 2011); and (4) the Guadalete Estuary (Fig. 4F), roughly circular and separated

* Corresponding author.

E-mail address: ruizmu@uhu.es (F. Ruiz).

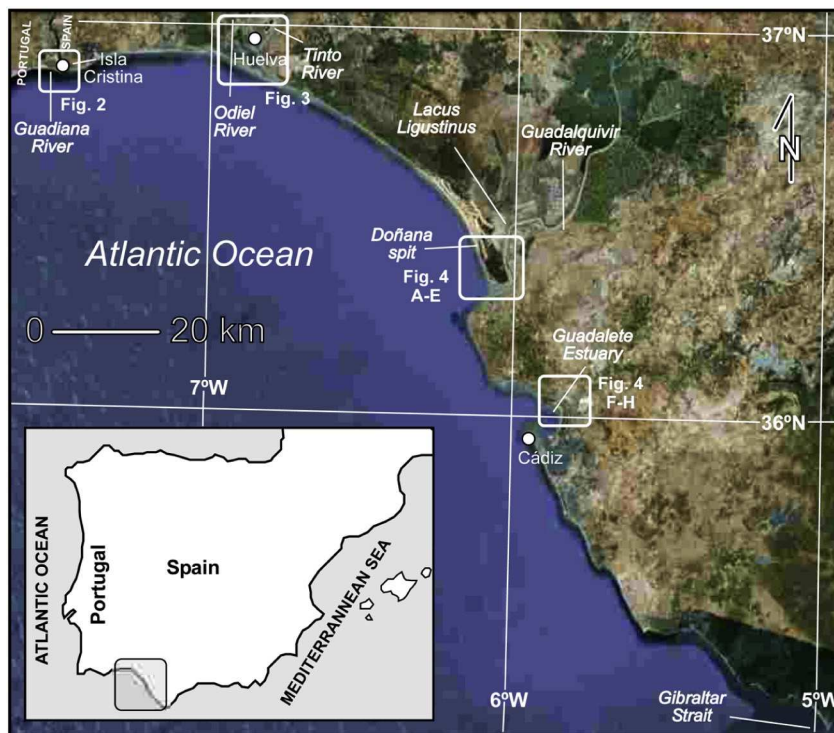


Fig. 1. Satellite image of the southwestern Spanish coast, with location of the four studied estuaries.

from the sea by a sedimentary spit (Dabrio et al., 2000). These and other minor estuaries are separated from each other by sandy beaches and Pleistocene cliffs in interfluvial areas.

2.2. The tectonic setting: Holocene tsunamis in SW Spain

The southwestern coast of Spain is located near the Africa-Eurasia plate boundary. This tectonic boundary extends from the Azores Archipelago to the Gibraltar Strait, with a complex interplate domain characterized by different ridges, seamounts (e.g. Gorringer Bank) and depressions (e.g. Horseshoe abyssal plain) (Omira et al., 2010). This boundary has been the source area of earthquakes of different magnitudes, some of them tsunami-causing, during pre-historical and historical times (Campos, 1992). Sixteen tsunamis have been recorded during the last 2300 years (Galbis, 1932; Campos, 1991) including the AD 1755 Great Lisbon earthquake (MSK intensity: VIII–IX; M_w : 8.5 ± 0.3 ; Baptista et al., 1998; Soares and Arroyo, 2004) and the related tsunami (Hindson et al., 1999; Blanc, 2008; Lima et al., 2010), one of the most devastating phenomena to have ever occurred in this area.

During the last decade, several papers have studied the prehistoric and historic Holocene record of these tsunamis in southwestern Spain, based on a multidisciplinary analysis of sediment cores or geomorphic evidences (e.g. Ruiz et al., 2004, 2005; Scheffers and Kelletat, 2005; Morales et al., 2008; Ruiz et al., 2008; Gràcia et al., 2010; Lario et al., 2011; Cuen et al., 2013). Nevertheless, the calibrated ages of these events require a reassessment due to the publication of new data concerning the reservoir effect in this area (e.g., Soares, 2010).

3. Methodology

In a first step, numerous historical maps and references were reviewed to deduce the palaeogeographical changes derived from the AD 1755 tsunami, with special attention to the Guadiana River mouth (see Section 4.1). These maps were selected from the General Archives of Sevilla and Simancas (Spain). In addition, the available literature on Holocene tsunamis affecting southwestern Spain and Portugal was analysed. The geological record was compared with new data on

modelling tsunami propagation in this area (e.g. Periañez and Abril, 2013).

A new reservoir effect (see Soares, 2010 for a more detailed explanation) has been applied to different radiocarbon datings obtained in three estuaries of southwestern Spain (Table 1: Guadiana, Guadalquivir and Guadalete). A $\Delta R = -135 \pm 20$ ^{14}C yr was used for samples with <2500 yr BP (conventional ^{14}C shell dates), whereas a $\Delta R = 100 \pm 100$ ^{14}C yr was used for samples with ages between 2500 and 4000 yr BP (also conventional ^{14}C shell dates). New data on reservoir effects are necessary to calibrate estuarine samples with ages between 4000 and 7000 yr BP.

Results have been compared with those extracted from abyssal cores by Gràcia et al. (2010). This comparison allows us to obtain an approximation to the recurrence period of tsunamis in this area during the last 7000 years.

4. Morphosedimentary imprints of past tsunamis: human implications

4.1. Guadiana River mouth

At present, the main channel of the Guadiana River marks the border between Spain and Portugal. On the Portuguese side, a large spit with a long jetty protects the town of Vila Real do Santo Antonio. The Spanish side presents several elongated, sandy spits that protect numerous marsh bodies crossed by the Carreras channel (Fig. 2A) and numerous distributary and ebb tidal channels. This general pattern is derived from a progressive infilling of the innermost areas due to the growing of an initial barrier-island system in a W–E direction during the last 3000 years (Morales, 1997).

Available historical maps only provide a general perspective on the geomorphological effects of the AD 1755 tsunami (Fig. 2B; General Archive of Simancas). In the Guadiana River mouth, the old channel was partially filled, whereas a new channel was created on the Portuguese side (Gozálvez, 2002). These geomorphic changes might be due to the rupture of sand bars and spits on the Portuguese side, the subsequent sediment redistribution, and the emergence of new sand

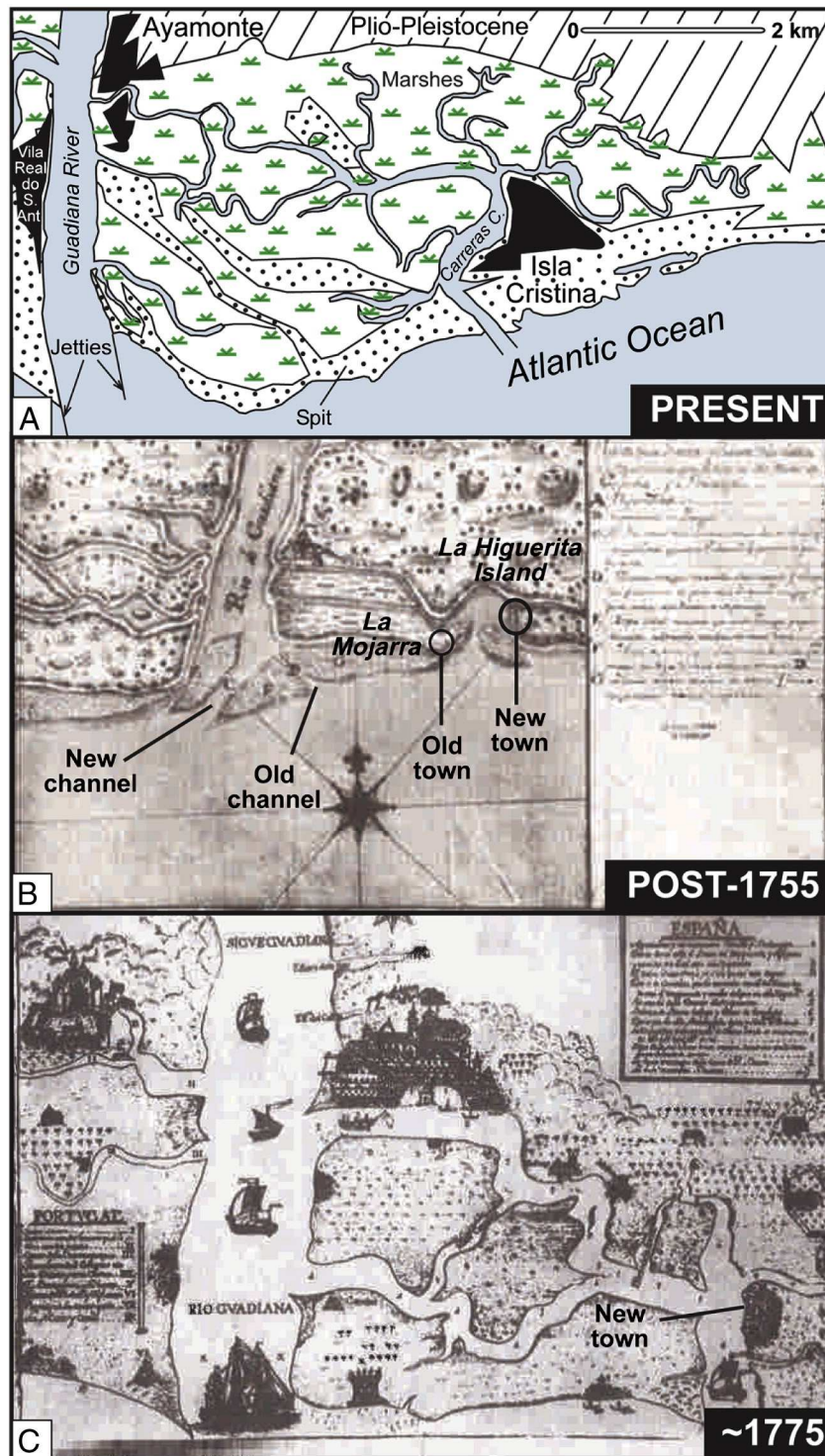


Fig. 2. Guadiana River Estuary. A: Main geomorphological features (modified from Morales, 1997); B: Historical map of the Guadiana mouth about 1760 (General Archive of Simancas); C: Historical map of the Guadiana mouth about 1775 (General Archive of Sevilla).

bars above the swash platform in the open intertidal zones close to the Spanish side (see Morales et al., 2006 for a more detailed description of these beds in recent environments). Consequently, the geomorphic changes derived from this tsunami 'redrew' an international border.

In addition, La Mojarra zone (Fig. 2B) was an important centre of fisheries (tuna, sardines) between AD 1720 and 1755 (Miravent, 1933). The AD1755 tsunami flooded this supratidal area and eroded the adjacent spit and beaches. This disaster caused more than 1000 deaths in this area

and the transfer of these activities in 1756 to the Higuera Island, a more protected environment that coincides with the present-day Isla Cristina village (Gozálvez, 1988). Some creeks located near this island were filled and several small islands disappeared (Ménanteau et al., 2006).

During the year 1775, the external spits of the Spanish side showed a remarkable expansion and the barrier island located on the western bank of the present-day Carreras channel (Fig. 2B) was attached to the western spit (Fig. 2C; General Archive of Sevilla). This growth was

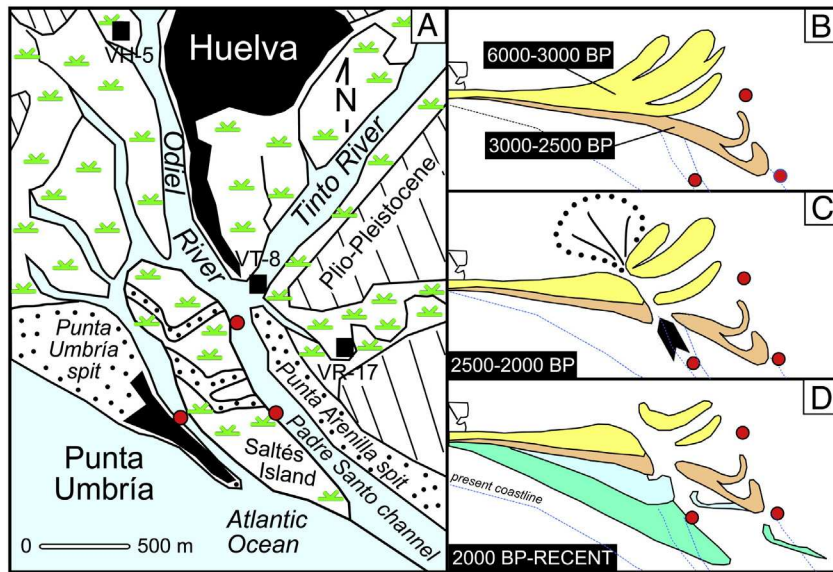


Fig. 3. Tinto–Odiel River Estuary. A: Main geomorphological features. Circles indicate geographical references for Fig. 3B–C–D. VH-5, VT-8, VR-18: examples of sediment cores with tsunamigenic layers (extracted from Morales et al., 2008); B–C–D: geomorphological evolution of Punta Umbría spit during the last 6000 years. Modified from Rodríguez-Vidal (1987).

clearly controlled by the W–E littoral drift currents and the Guadiana sediment supplies, not regulated by dams at that time.

4.2. Tinto–Odiel Estuary

The Tinto–Odiel Estuary is a 25 km long incised valley underlain by Plio–Pleistocene marine and fluvial sediments. A cross-section of the outer zone shows two main (Punta Umbría and Punta Arenillas) sandy spits (Fig. 3A) separated by the Saltés Island, a salt-marsh

sediment body comprising old spits. This central island delineates the deeper Padre Santo channel, which is the main passage to the Huelva harbour, and the narrower Punta Umbría channel.

In this estuary, the maximum of the Holocene transgression (7000–6500 yr BP; Zazo et al., 1994) marked the beginning of key geomorphological features (e.g. Punta Umbría spit) that controlled its subsequent evolution. In an early stage (6000–2500 yr BP), the Punta Umbría spit emerged and prograded southeastward with the progressive addition of attached beach berms. In this phase, several

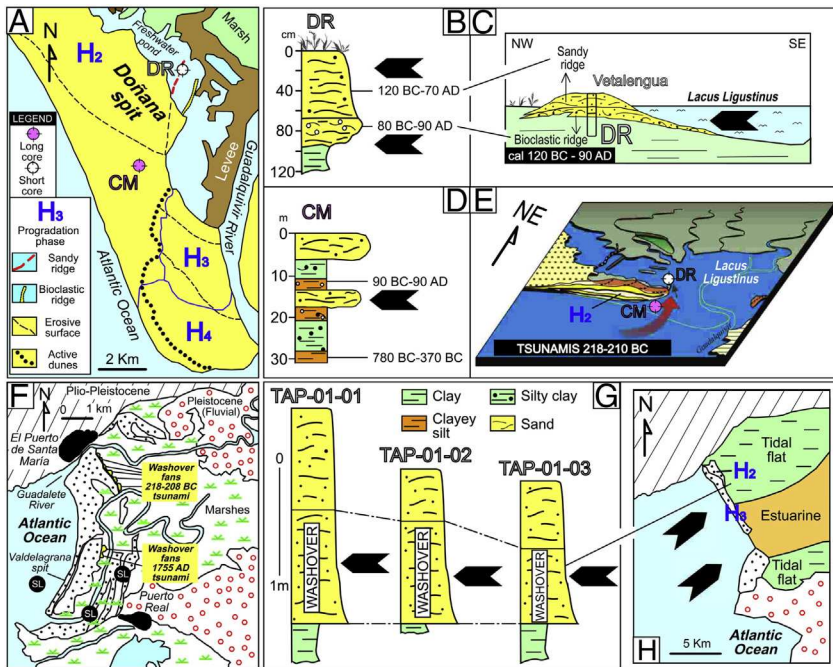


Fig. 4. Guadalquivir River Estuary (A–E) and Guadalete River Estuary (F–H). A: Main geomorphological characteristics of the river mouth. B: Sedimentological features of short sediment core D, including the calibrated ages of two tsunamigenic layers (modified from Ruiz et al., 2004). C: Interpretative cross-section of this area during Roman time (modified from Rodríguez-Vidal et al., 2011). D: Sedimentological features of long sediment core, including two calibrated ages (modified from Rodríguez-Vidal et al., 2011). E: Palaeogeographical reconstruction of the Guadalquivir mouth (218–209 BC) (modified from Rodríguez-Vidal et al., 2011). F: Main geomorphological features of the Guadalete Estuary (modified from Luque et al., 2002); SL: emerged trenches or subtidal cores with tsunamigenic, shelly layers (data from Gutiérrez-Más et al., 2009b; Gutiérrez-Más, 2011). G: washover fans deposited by the 218–209 BC tsunami, with a draw top limited by sedimentological and palaeontological features (modified from Luque et al., 2002). H: Palaeogeographical reconstruction of the Guadalete Estuary (218–209 BC; modified from Luque et al., 2002), with location of cores. Panels B, D, F, G and H share their legends.

Table 1

Radiocarbon calibrated ages of tsunamigenic layers in the abyssal plain of southwestern Iberia and three estuaries of southwestern Spain.

Zone	Laboratory	Number	Uncalibrated radiocarbon age (yr BP + 1 σ)	ΔR	2 σ calibrated age (cal. yr BP)	Reference	Fig. 5
Abyssal plain	NOSAMS-WHOI	49086	6970 \pm 45	95 \pm 15	7285–7480	Gràcia et al. (2010)	1
	NOSAMS-WHOI	49065	6770 \pm 40	95 \pm 15	7110–7310	Gràcia et al. (2010)	2
	NOSAMS-WHOI	49079	6770 \pm 40	95 \pm 15	7110–7310	Gràcia et al. (2010)	3
	NOSAMS-WHOI	49085	6150 \pm 45	95 \pm 15	6360–6615	Gràcia et al. (2010)	4
	NOSAMS-WHOI	49078	6100 \pm 45	95 \pm 15	6300–6540	Gràcia et al. (2010)	5
	NOSAMS-WHOI	49064	5200 \pm 70	95 \pm 15	5300–5590	Gràcia et al. (2010)	6
	NOSAMS-WHOI	52122	2790 \pm 35	95 \pm 15	2300–2530	Gràcia et al. (2010)	7
	NOSAMS-WHOI	49063	2530 \pm 100	95 \pm 15	1850–2320	Gràcia et al. (2010)	8
	No data	No data	No data	No data	755–1270 (extrapolated)	Gràcia et al. (2010)	9
	NOSAMS-WHOI	49084	1200 \pm 60	95 \pm 15	540–780	Gràcia et al. (2010)	10
Tinto–Odiel Estuary	LDR-BU	VT-15	3240 \pm 100	100 \pm 100	2650–3330	Pendón et al. (1998)	11
	LDR-BU	VR-3	3090 \pm 60	100 \pm 100	2430–3070	Pendón et al. (1998)	12
	LDR-BU	VH-5	1800 \pm 80	(–135 \pm 20)	1310–1680	Pendón et al. (1998)	13
	Geochron Laboratory	GX-31680	1680 \pm 60	(–135 \pm 20)	1250–1510	Morales et al. (2008)	14
	LDR-BU	VT-8	1620 \pm 70	(–135 \pm 20)	1160–1480	Pendón et al. (1998)	15
	Geochron Laboratory	GX-31681	1190 \pm 60	(–135 \pm 20)	720–1000	Morales et al. (2008)	16
	Geochron Laboratory	GX-31682	910 \pm 60	(–135 \pm 20)	510–710	Morales et al. (2008)	17
	LDR-BU	VT-14	440 \pm 160	(–135 \pm 20)	0–460	Pendón et al. (1998)	18
	LDR-BU	VR-17	300 \pm 80	(–135 \pm 20)	Uncalibrated	Pendón et al. (1998)	19
Guadalquivir Estuary	Beta Analytic Inc.	B-2279	3679 \pm 48	100 \pm 100	3210–3770	Ruiz et al. (2005)	20
	Beta Analytic Inc.	B-228880	3550 \pm 40	100 \pm 100	3030–3590	Pozo et al. (2010)	21
	Beta Analytic Inc.	B-154087	3460 \pm 40	100 \pm 100	2920–3460	Ruiz et al. (2005)	22
	Beta Analytic Inc.	B-154084	3380 \pm 40	100 \pm 100	2835–3370	Ruiz et al. (2005)	23
	Beta Analytic Inc.	B-145202	2570 \pm 70	100 \pm 100	1820–2420	Rodríguez-Ramírez and Camacho (2008)	24
Guadalete Estuary	Beta Analytic Inc.	B-88022	2487 \pm 70	(–135 \pm 20)	2100–2530	Zazo et al. (1994)	25
	University of Granada	No data	3504 \pm 45	100 \pm 100	2970–3540	Gutiérrez-Más (2011)	26
	Geochron Laboratory	GX-27986	2340 \pm 40	(–135 \pm 20)	2000–2280	Luque et al. (2002)	27
	University of Granada	No data	2058 \pm 40	(–135 \pm 20)	1680–1910	Gutiérrez-Más (2011)	28
	University of Granada	No data	1960 \pm 110	(–135 \pm 20)	1400–1930	Gutiérrez-Más (2011)	29
	University of Granada	No data	1910 \pm 60	(–135 \pm 20)	1460–1790	Gutiérrez-Más (2011)	30
	University of Granada	No data	1670 \pm 60	(–135 \pm 20)	1245–1500	Gutiérrez-Más (2011)	31
	University of Granada	No data	1590 \pm 60	(–135 \pm 20)	1140–1400	Gutiérrez-Más (2011)	32

curved spits were created near the end of this main spit, such as the current Saltés Island (Fig. 3B; Rodríguez-Vidal, 1987). The intermediate stage (Fig. 3C: 2500–2000 yr BP) is characterized by the breakdown of this spit, with the generation of an inner washover fan and the appearance of the Punta Umbría inlet. These geomorphological changes could have been induced by the 218–209 BC tsunamis, the only high-energy events that occurred during this historical period (Galbis, 1932). In a final stage (Fig. 3D: 2000 yr BP–recent), the littoral drift currents caused the progradation of beaches attached to the southeastern corner of the spit, whereas the tidal fluxes associated to the new inlet generated small spits linked to the Saltés Island. These spits are partially preserved nowadays (Fig. 3A).

Other tsunamigenic imprints have been found in the innermost areas of this estuary. Several sediment cores collected across the different estuarine environments (marsh, channel margin, channel, spit) contain bioclastic layers (e.g. Fig. 3A: cores VH-5, VT-8 or VR-17). These beds exhibit an erosional base, a fining-upwards sequence, a mixing of both estuarine and marine faunas and have been interpreted as tsunamigenic layers (Morales et al., 2008). The inner location of some of them (e.g. VH-5) would indicate a complete propagation of the tsunami waves along the whole estuary during these events.

4.3. Guadalquivir Estuary

The Guadalquivir River (560 km long) is partly blocked by two (Doñana and La Algaída) sandy spits (Fig. 4A) in the lower reach, resulting in a large estuary (1800 km²). Four regional spit systems have been defined in the Holocene (H₁: 6900–4500 cal. yr BP; H₂: 4200–2600 cal. yr BP; H₃: 2300–1100 cal. yr BP; H₄: 1000 cal. yr BP to the present) divided by erosional phases at 4500–4200 cal. yr BP, 2600–2300 cal. yr BP and 1100–1000 cal. yr BP (Zazo et al., 1994; Rodríguez-Ramírez et al., 1996).

The 218–209 BC tsunami caused a strong geomorphic disturbance (Ruiz et al., 2004; Rodríguez-Vidal et al., 2011) in both former spits and the adjacent *Lacus Ligustinus*, a brackish lagoon detailed by the Roman chroniclers Strabo and Mela in the first historical descriptions of this estuary (García-Bellido, 1987). Several geomorphological imprints are linked to this high-energy event:

- i Beach erosion and shoreline retreat in the external side of the Doñana spit, with the presence of a distinctive erosional surface along the southeastern part of this bed (Rodríguez-Ramírez et al., 1996).
- ii Accumulation of bioclastic ridges along or very close to the lagoon margins (Fig. 4B: lower arrow) by tsunami waves or post-tsunami tidal fluxes. These ridges were deposited by this tsunami and other older high-energy events in the innermost areas of the lagoon (e.g. Ruiz et al., 2008; Pozo et al., 2010). They are elongated (3–6 km), with a narrow width (20–30 m) and low thickness (0.5–0.7 m). These silts and sands containing bioclasts display an erosional base and a bimodal grain size distribution. Its mineralogy is composed of phyllosilicates (20–65%; mean: 38.8%), quartz (9–70%; mean: 28.2%) and calcite (12–40%; mean: 20.3%), with illite (mean: 53%) as dominant clay mineral. Both macrofauna and microfauna include estuarine and marine reworked species.
- iii Deposition of reworked sandy ridges (Fig. 4B: upper arrow), derived from the direct erosion of the Doñana spit, a late tidal redistribution and finally deposited close to the *Lacus Ligustinus* margin (Fig. 4C). These spit-like beds are formed by yellow, fine to medium sands very rich in quartz (>75%), with very scarce fauna. Other sandy ridges have been observed in the northwestern part of the old *Lacus Ligustinus* (Ruiz et al., 2005). Both bioclastic and sandy ridges represent the only heights in this area (2–2.5 m above the marsh level; Ruiz et al., 2004). They remained emerged during the fluvial flooding underwent by the

- estuary, with the occurrence of numerous freshwater ponds so-called 'lucios' (Fig. 4A). An unexpected ecological consequence is its use as shelter for birds and other autochthonous wildlife (cows, horses) during these wet intervals.
- iv Deposition of subtidal sandy layers (Fig. 4D: arrow) in infralittoral environments located near the lagoon mouth (Fig. 4E). These layers (>3 m thickness) show very similar features to the previously described sandy ridges (medium sands with high percentages of quartz and absence of microfauna and macrofauna), indicating a common origin (e.g., the erosion of the Doñana spit; Pozo et al., 2008).
 - v Erosion of the pre-218 BC eastern ridges of Doñana and La Algaida spit-barriers (Rodríguez-Vidal et al., 2011) and shoals by incoming tsunami waves and mainly by the backwash currents. This action created a channelled morphology, with small cliffs at right angles to the coastline, which are partially preserved today. Relict high-energy beaches were attached to the new cliff morphologies composed of fine sands with numerous bioclasts, rock fragments and pebbles.
 - vi Erosion of the first line of foredunes and former dune ridges of the great sand barrier of Doñana, which nevertheless protected the coastal and tidal lowlands (Rodríguez-Ramírez et al., 1996). Accordingly, transgressive dunes were reactivated and migrated inland, toward the inner estuary (Rodríguez-Vidal et al., 2011), as large parabolic sand sheets.

The palaeogeographical and geomorphological reconstruction of the post-tsunami littoral landscape (Rodríguez-Vidal et al., 2011) coincides with the earliest historical description of the estuary, made by the Roman chronicler Strabo in his work *Geographica*, written between 29 and 7 years BC. La Algaida spit-barrier includes the unique pre-Roman settlement (sanctuary) documented in this coastal area (7th–3rd centuries BC: Blanco and Corzo, 1983). This ancient settlement was abandoned approximately at the date of the tsunami, when this sandy barrier became an island (Rodríguez-Ramírez et al., 1996). Later, in the 1st century AD, and when the connection with the continent was re-established, the Romans installed a saltworks on the eastern coast, sheltered from wave action (Esteve Guerrero, 1952).

New tsunami models attempting to reproduce the 218–209 BC tsunami indicate that such a tsunami would erode the southern shore of the Doñana spit and nearby sectors, with the subsequent sedimentary spreading on the western area of the roman *Lacus Ligustinus* (Periañez and Abril, 2013). According to this new model, the tsunami could hardly produce any severe damage in the innermost areas of this old brackish lagoon. These data are in good agreement with the geological and historical records, which are compatible with geomorphic changes and human settlement near the lagoon outlet (Rodríguez-Vidal et al., 2011).

4.4. Guadalete Estuary

This estuary contains wide marshes surrounded by Plio–Pleistocene marine and fluvial formations and protected by the Valdellagrana spit (Fig. 4F), a complex sedimentary system that includes three spit systems with equivalent sediment bodies also described in the Guadalquivir Estuary (H₂ to H₄; Dabrio et al., 2000). Different sedimentological and geomorphological imprints of past tsunamis have been observed in this area:

- a Washover fans. These beds have limited length (350–400 m), width (200–300 m) and height (<4 m). These sedimentary units (<1.5 m thickness) are derived from the erosion of sandy spits and display a sharp, erosional contact with underlying flat facies (Dabrio et al., 1998a,b; Luque et al., 2001, 2002). They are composed of yellow, poorly sorted coarse-medium sands with high percentages of quartz and bioclast fragments of molluscs, echinoids and bryozoans (Fig. 4G; see location in Fig. 4H). These washover fans were generated by the 218–209 BC (Fig. 4H; Luque et al., 2002) and AD 1755 tsunamis.

- b Shelly sandy layers observed in both subtidal and emerged zones (Fig. 4F: SL; Gutiérrez-Más et al., 2009a,b; Gutiérrez-Más, 2011). Biogenic clasts consist of bivalve shells (mainly *Glycymeris*), sometimes imbricated, with evidence of abrasion, impact marks and dissolution. These medium to fine bioclastic sands are poorly sorted and can be arranged in surface bands (3–15 m long, 1–3 m wide). The application of new reservoir effect data (Soares, 2010) allows us to link most of these high-energy beds with prehistoric (>3000 cal. yr BP; Pozo et al., 2010) and historic (AD 382–395) tsunamis.
- c Destruction of beaches connecting Cádiz city (Fig. 1) with the mainland (Campos, 1992). A similar tombolo breaking was caused by the 2004 Indian Ocean tsunami in the small low-lying atoll islands of the Maldives (Kench et al., 2008). The AD 1755 tsunami caused severe damage in this area, with run-ups up to 5 m (Baptista et al., 1998; Blanc, 2008). In El Puerto de Santa María city (Fig. 4F), this tsunami left five dead, flooded houses and stores near the Guadalete River and dragged boats landward (Luque, 2008). In Cádiz city, an important part of the town walls, defensive bastions, port infrastructure and saltworks were destroyed and beaches were eroded (Campos, 1992).

5. The tsunami recurrence in SW Spain

Calibrated ages of tsunamigenic layers documented in offshore marine environments (Gràcia et al., 2010) and estuaries (see Ruiz et al., 2005; Morales et al., 2008; Lario et al., 2011, for a review), as well as the application of a new reservoir effect (Soares, 2010; Soares and Martins, 2010) enabled us to estimate the recurrence period of tsunami events in the Gulf of Cádiz region.

During the last 7000 years, the effects of prehistorical and historical tsunamis were identified in the geological record of abyssal cores and estuarine deposits. The three older tsunamis deposited three turbidities in deep environments (Fig. 5: ~7300–7100 cal. yr BP; ~6600–6300 cal. yr BP; ~5600–5300 cal. yr BP), whereas the estuarine record needs additional research on the reservoir effect of the 7000–4000 yr BP interval to elucidate the calibrated ages of some bioclastic or sandy layers observed in three estuaries (Tinto–Odiel, Guadalquivir and Guadalete), attributed either to tsunamis or extreme wave events (see Lario et al., 2011 for a review).

The sedimentary record of other additional tsunamis (~3300–3000 cal. yr BP; 218–209 BC; 60 BC; AD 382; AD 889; AD 949; AD 1531; and AD 1755) caused strong sedimentary signatures in the southwestern Spanish estuaries but some of them are not recorded in deep cores. The historical ages of the last five tsunamis were positioned at the end of the 2 σ -calibrated radiocarbon age interval of numerous tsunamigenic layers, or they are older than this probability interval (Fig. 5).

The final perspective of new prehistoric calibrated ages and historical evidences (Fig. 5) will indicate a 'tsunamigenic interval' each 700–1000 years in this area, with possible intermediate tsunamis (e.g. AD 382; AD 1531). This recurrence period (700–1000 years) is shorter than the period proposed (1200–1500 years) by Lario et al. (2011) for damaging tsunamis in the Gulf of Cádiz or the recurrence period deduced by Gràcia et al. (2010) for great earthquakes (1800 years) in the same area. Nevertheless, Matias et al. (2013) proposed recently a similar recurrence period (700 years) for events of $M_w = 8$ in this area, using fault slip-rates inferred from the thin-sheet neotectonic modelling of Cunha et al. (2012). According to these authors, large earthquakes will happen clustered in time due to fault interaction. This possibility could explain the historical 'tsunamigenic intervals' (e.g. 218–209 BC; AD).

6. Conclusions

The southwestern Spanish estuaries are excellent geological archives of both prehistoric and historical tsunamis, with a wide

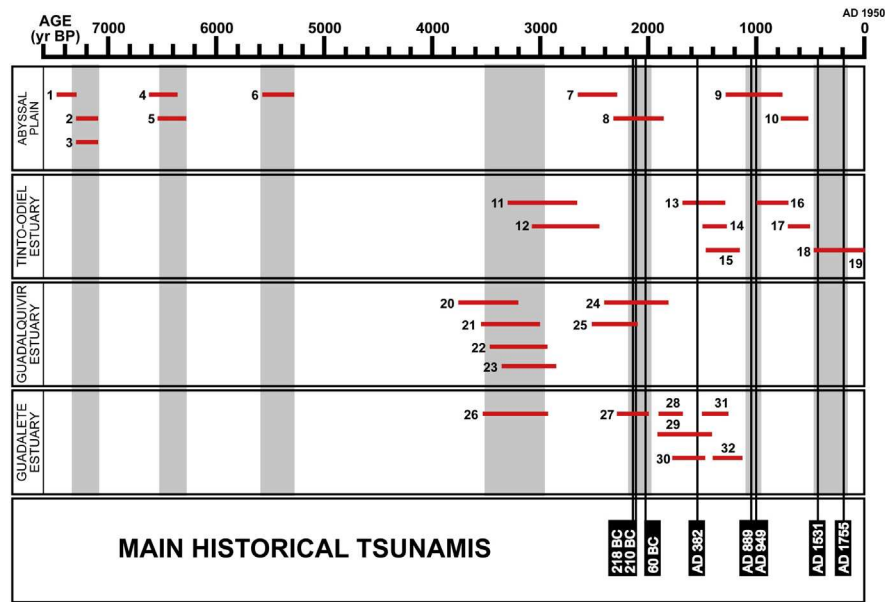


Fig. 5. Calibrated ages of tsunamigenic layers in deep cores and three estuaries of southwestern Spain. Original data from Luque et al. (2002), Ruiz et al. (2004, 2005, 2008), Morales et al. (2008), Gutiérrez-Más et al. (2009a,b), Pozo et al. (2010), Gràcia et al. (2010), Rodríguez-Vidal et al. (2011), Gutiérrez-Más (2011) and Lario et al. (2011).

set of sedimentological and geomorphological imprints. The most frequent features are beach erosion with shoreline retreat, breaking or overwash of sandy spits and deposition of bioclastic layers.

During the last 4000 years, two historical tsunamis (218–209 BC and AD 1755) are revealed as extremely violent events which caused most of these geomorphic imprints. The geomorphological record of other tsunamis (3300–3000 cal. yr BP, AD 382, AD 1531) is more restricted.

The 218–209 BC and AD 1755 tsunamis caused substantial changes in the coastal settlements and their adjacent landscapes, with the creation of new waterways and/or the relocation of fishery activities. They clearly conditioned the further geographical development of these areas. In addition, the AD 1755 tsunami was accompanied by high mortality and probably by important injury among the exposed population.

The application of a new marine reservoir effect and additional data derived from new tectonic models suggest a recurrence period of 700–1000 years for a 'tsunamigenic interval' along this Atlantic shore.

Acknowledgements

This research was funded by the Spanish–FEDER Projects CTM2006-06722/MAR, CGL2006-01412/BTE, CGL2010-15810/BTE and CGL2012-30875, an Excellence Project of the Andalucía Board (SEJ-4770) funded by EU, a Project funded by the Fundação para a Ciência e a Tecnologia (PTDC/CTE-GIX/110205/2009) and three Research Groups of the Andalucía Board (RNM-238, RNM-293, and RNM-349). We thank reviewers and guest-editors for helpful comments. This work is a contribution to the IGCPs 526 (risks, resources, and record of the past on the continental shelf), 567 (Earthquake Archaeology and Palaeoseismology), and 588 (preparing for coastal change).

References

Baptista, M.A., Heitor, S., Miranda, J.M., Mendes Victor, L., 1998. The 1755 Lisbon tsunami: evaluation of tsunami parameters. *J. Geodyn.* 25, 143–157.
 Blanc, P.L., 2008. The tsunami in Cádiz on 1 November 1755: a critical analysis of reports by Antonio de Ulloa and by Louis Godin. *Compt. Rendus Geosci.* 340, 251–261.
 Blanco, A., Corzo, R., 1983. Monte Algaida. Un santuario púnico en la desembocadura del Guadalquivir. *Historia* 16 (87), 122–128.
 Campos, M.L., 1991. Tsunami hazard on the Spanish coasts of the Iberian peninsula. *Sci. Tsunami Hazards* 9, 83–90.
 Campos, M.L., 1992. El riesgo de tsunamis en España. Análisis y valoración geográfica, vol. 9. Monografías Instituto Geográfico Nacional, Madrid (204 pp.).

Choowong, M., Phantuwongraj, S., Charoentitir, T., Chutakositkanon, V., Yumuand, S., Charusiri, P., 2009. Beach recovery after 2004 Indian Ocean tsunami from Phang-nga, Thailand. *Geomorphology* 104, 134–142.
 Cunha, T.A., Matias, L.M., Terrinha, P., Negredo, A., Rosas, F., Fernandes, R.M.S., Pinheiro, L.M., 2012. Neotectonics of the SW Iberia margin, Gulf of Cadiz and Alboran Sea: a reassessment including recent structural, seismic and geodetic data. *Geophys. J. Int.* 188, 850–872.
 Cuven, S., Paris, R., Falvard, S., Miot-Noirault, E., Benbakkar, M., Schneider, J.-L., Billy, I., 2013. High-resolution analysis of a tsunami deposit: case-study from the 1755 Lisbon tsunami in southwestern Spain. *Mar. Geol.* 337, 98–111.
 Dabrio, C.J., Zazo, C., Lario, J., Goy, J.L., Sierro, F.J., Borja, F., González, J.A., Flores, J.A., 1998a. Holocene incised-valley fills and coastal evolution in the Gulf of Cádiz (southern Spain). *Mediterr. Black Sea Subcommission Newsl.* 20, 45–48.
 Dabrio, C.J., Goy, J.L., Zazo, C., 1998b. The record of the tsunami produced by the 1755 Lisbon earthquake in Valdelagrana spit (Gulf of Cádiz, southern Spain). *Geogaceta* 23, 31–34.
 Dabrio, C.J., Zazo, C., Goy, J.L., Sierro, F.J., Borja, F., Lario, J., González, J.A., Flores, J.A., 2000. Depositional history of estuarine infill during the last post-glacial transgression (Gulf of Cadiz, southern Spain). *Mar. Geol.* 162, 381–404.
 Esteve Guerrero, M., 1952. Sanlúcar de Barrameda (Cádiz): fábrica de salazón romana en La Algaida. *Not. Arqueológico Hispánico* 1–3, 126–133.
 Fagherazzi, S., Du, X., 2008. Tsunamigenic incisions produced by the December 2004 earthquake along the coasts of Thailand, Indonesia and Sri Lanka. *Geomorphology* 99, 120–129.
 Galbis, R.J., 1932. Catálogo sísmico de la zona comprendida entre los meridianos 58° E y 20° W de Greenwich y los paralelos 45° y 25° N. Dirección General del Instituto Geográfico, Catastral y de Estadística, Madrid.
 García-Bellido, A., 1987. La España del siglo primero de nuestra era (según P. Mela y C. Plinio). Colección Austral.Espasa Calpe, Madrid.
 General Archive of Sevilla, 1775. Plano de la desembocadura del río Guadiana.
 General Archive of Simancas, 1764. Plano de la barra y puerto de la ciudad de Ayamonte que divide los dos Reinos de España y Portugal.
 Goff, J., Pearce, S., Nichol, S.L., Ghabuê-Goff, C., Horrocks, M., Strotz, L., 2010. Multi-proxy records of regionally-sourced tsunamis, New Zealand. *Geomorphology* 118, 369–382.
 Goto, K., Takahashi, J., Oie, T., Imamura, F., 2011. Remarkable bathymetric change in the nearshore zone by the 2004 Indian Ocean tsunami: Kirinda Harbor, Sri Lanka. *Geomorphology* 127, 107–116.
 Gozávez, J.L., 1988. Los orígenes de Isla Cristina. El impulso pesquero. Ilmo. Ayuntamiento de Isla Cristina.
 Gozávez, J.L., 2002. Un ensayo de reconstrucción de la línea de costa histórica: Ayamonte, siglos XVII–XX. *J. Hist. Ayamonte* VI, 51–82.
 Gràcia, E., Vizcaino, A., Escutia, C., Asioli, A., Rodés, A., Pallàs, R., García-Orellana, J., Lebreiro, S., Goldfinger, C., 2010. Holocene earthquake record offshore Portugal (SW Iberia): testing turbidite palaeoseismology in a slow-convergence margin. *Quat. Sci. Rev.* 29, 1156–1172.
 Gutiérrez-Más, J.M., 2011. *Glycymeris* shell accumulations as indicators of recent sea-level changes and high-energy events in Cádiz Bay (SW Spain). *Estuar. Coast. Shelf Sci.* 92, 546–554.
 Gutiérrez-Más, J.M., López-Arroyo, J., Morales, J.A., 2009a. Recent marine lithofacies in Cádiz Bay (SW Spain): sequences, processes and control factors. *Sediment. Geol.* 218, 31–47.
 Gutiérrez-Más, J.M., Juan, C., Morales, J.A., 2009b. Evidence of high-energy events in shelly layers interbedded in coastal Holocene sands in Cádiz Bay (south-west Spain). *Earth Surf. Process. Landf.* 34, 810–823.

- Hindson, R., Andrade, C., Parish, R., 1999. A microfungal and sedimentary record of environmental change within the late Holocene sediments of Boca do Rio (Algarve, Portugal). *Geol. Mijnb.* 77, 311–321.
- Kench, P.S., Nichol, S.L., Smithers, S.G., McLean, R.F., Brander, R.W., 2008. Tsunami as agents of geomorphic change in mid-ocean reef islands. *Geomorphology* 95, 361–383.
- Lario, J., Zazo, C., Goy, J.L., Silva, P.G., Bardají, T., Cabero, A., Dabrio, C.J., 2011. Holocene palaeotsunami catalogue of SW Iberia. *Quat. Int.* 242, 196–209.
- Liew, S.C., Gupta, A., Wong, P.P., Kwok, L.K., 2010. Recovery from a large tsunami mapped over time: the Aceh coast, Sumatra. *Geomorphology* 114, 520–529.
- Lima, V.V., Miranda, J.M., Baptista, M.A., Catalao, J., González, M., Otero, L., Olabarrieta, M., Álvarez-Gómez, J.A., Carretero, E., 2010. Impact of a 1755-like tsunami in Huelva, Spain. *Nat. Hazards Earth Syst. Sci.* 10, 139–148.
- Luque, L., 2008. El impacto de eventos catastróficos costeros en el litoral del Golfo de Cádiz. *Rev. Atlántica Mediterr. Prehist. Arqueol. Soc.* 10, 131–153.
- Luque, L., Lario, J., Zazo, C., Goy, J.L., Dabrio, C.J., Silva, P.G., 2001. Tsunami deposits as palaeoseismic indicators: examples from the Spanish coast. *Acta Geol. Hisp.* 3–4, 197–211.
- Luque, L., Lario, J., Civiş, J., Silva, P.G., Zazo, C., Goy, J.L., Dabrio, C.J., 2002. Sedimentary record of a tsunami during Roman times, Bay of Cádiz. *J. Quat. Sci.* 17, 623–631.
- Mascarenhas, A., 2006. Extreme events, intrinsic landforms and humankind: post-tsunami scenario along Nagore–Velankanni coast, Tamil Nadu, India. *Curr. Sci.* 90–99, 1195–1201.
- Matias, L.M., Cunha, T., Annunziato, A., Baptista, M.A., Carrilho, F., 2013. Tsunamigenic earthquakes in the Gulf of Cádiz: fault model and recurrence. *Nat. Hazards Earth Syst. Sci.* 13, 1–13.
- Ménanteau, L., Chadenas, C., Choblet, C., 2006. Les marais du Bas-Guadiana (Algarve, Andalousie): emprise, déprise et reprise humaines. *Aestuaria* 9, 309–331.
- Miravent, J., 1933. Memoria sobre la fundación y progresos de la Real Isla de la Higuierita (Reprinted by Artes Gráficas M. Vázquez, Isla Cristina, Spain).
- Monecke, K., Finger, W., Klarer, D., Kongko, W., McAdoo, B.G., Moore, A.L., Sudrajat, S.U., 2008. A 1000-year sediment record of tsunami recurrence in northern Sumatra. *Nature* 455, 1232–1234.
- Morales, J.A., 1997. Evolution and facies architecture of the mesotidal Guadiana River delta (S.W. Spain–Portugal). *Mar. Geol.* 138, 127–148.
- Morales, J.A., Delgado, I., Gutiérrez-Mas, J.M., 2006. Sedimentary characterization of bed types along the Guadiana estuary (SW Europe) before the construction of the Alqueva dam. *Estuar. Coast. Shelf Sci.* 70, 117–131.
- Morales, J.A., Borrego, J., San Miguel, E.G., López-González, N., Carro, B., 2008. Sedimentary record of recent tsunamis in the Huelva estuary (southwestern Spain). *Quat. Sci. Rev.* 27, 734–746.
- Omira, R., Baptista, M.A., Miranda, J.M., Toto, E., Catita, C., Catalao, J., 2010. Tsunami vulnerability assessment of Casablanca–Morocco using numerical modelling and GIS tools. *Nat. Hazards* 54, 75–95.
- Paris, R., Wassmer, P., Sartohadi, J., Lavigne, F., Barthelemy, B., Desgages, E., Grancher, D., Baumert, P., Vautier, F., Brunstein, D., Gomez, C., 2009. Tsunamis as geomorphic crisis: lessons from the December 26, 2004 tsunamis in Lhok Nga, west Banda Aceh (Sumatra, Indonesia). *Geomorphology* 104, 59–72.
- Pendón, J.G., Morales, J.A., Borrego, J., Jiménez, I., López, M., 1998. Evolution of estuarine facies in a tidal channel environment SW Spain: evidence for a change from tide-to wave-dominance. *Mar. Geol.* 147, 43–62.
- Periañez, R., Abril, J.M., 2013. Modeling tsunami propagation in the Iberia–Africa plate boundary: historical events, regional exposure and the case-study of the former Gulf of Tartessos. *J. Mar. Syst.* 111–112, 223–234.
- Pozo, M., Carretero, M.I., Ruiz, F., Rodríguez Vidal, J., Cáceres, L.M., Abad, M., 2008. Caracterización mineralógica de facies sedimentarias de edad Pleistoceno superior–Holoceno en el Parque Nacional de Doñana (Huelva). Implicaciones paleoambientales. *Geotemas* 10, 953–956.
- Pozo, M., Ruiz, F., Carretero, M.I., Rodríguez Vidal, J., Cáceres, L.M., Abad, M., González-Regalado, M.L., 2010. Mineralogical assemblages, geochemistry and fossil associations of Pleistocene–Holocene complex siliciclastic deposits from the southwestern Doñana National Park (SW Spain): a palaeoenvironmental approach. *Sediment. Geol.* 225, 1–18.
- Rodríguez-Ramírez, A., Camacho, C.M., 2008. Formation of chenier plain of the Doñana marshland (SW Spain): observations and geomorphic model. *Mar. Geol.* 254, 187–196.
- Rodríguez-Ramírez, A., Rodríguez-Vidal, J., Cáceres, L.M., Clemente, L., Belluomini, G., Manfra, L., Improta, S., de Andrés, J.R., 1996. Recent coastal evolution of the Doñana National Park (SW Spain). *Quat. Sci. Rev.* 15, 803–809.
- Rodríguez-Vidal, J., 1987. Modelo de evolución geomorfológica de la flecha litoral de Punta Umbría, Huelva, España. *Cuaternario y Geomorfología* 1, 247–256.
- Rodríguez-Vidal, J., Ruiz, F., Cáceres, L.M., Abad, M., González-Regalado, M.L., Pozo, M., Carretero, M.I., Monge, A.M., Gómez, F., 2011. Geomarkers of the 218–209 BC Atlantic tsunami in the Roman *Lacus Ligustinus* (SW Spain): a palaeogeographical approach. *Quat. Int.* 242, 201–212.
- Ruiz, F., Rodríguez Ramírez, A., Cáceres, L.M., Rodríguez-Vidal, J., Carretero, M.I., Clemente, L., Muñoz, J.M., Yáñez, C., Abad, M., 2004. Late Holocene evolution of the southwestern Doñana National Park (Guadalquivir Estuary, SW Spain): a multivariate approach. *Palaeogeogr. Palaeoclimatol. Palaeoecol.* 204, 47–64.
- Ruiz, F., Rodríguez Ramírez, A., Cáceres, L.M., Rodríguez Vidal, J., Carretero, M.I., Abad, M., Ollas, M., Pozo, M., 2005. Evidence of high-energy events in the geological record: mid-Holocene evolution of the southwestern Doñana National Park (SW Spain). *Palaeogeogr. Palaeoclimatol. Palaeoecol.* 229, 212–229.
- Ruiz, F., Abad, M., Rodríguez-Vidal, J., Cáceres, L.M., González-Regalado, M.L., Carretero, M.I., Pozo, M., Gómez Toscano, F., 2008. The geological record of the oldest historical tsunamis in southwestern Spain. *Riv. Ital. Paleontol. Stratigr.* 114, 147–156.
- Salvany, J.M., Cruz Larrasoña, J., Mediavilla, C., Rebollo, A., 2011. Chronology and tectono-sedimentary evolution of the Upper Pliocene to Quaternary deposits of the lower Guadalquivir foreland basin, SW Spain. *Sediment. Geol.* 241, 22–39.
- Scheffers, A., Kelletat, D., 2005. Tsunami relics in the coastal landscape west of Lisbon, Portugal. *Sci. Tsunami Hazards* 23, 3–16.
- Siwar, C., Ibrahim, M.Z., Harizan, S.T.M., Kamaruddin, R., 2006. Impact of tsunami on fishing, aquaculture and coastal communities in Malaysia. *Proceedings Persidangan Antarabangsa Pembangunan Aceh, UKM Bangi, Malaysia*, pp. 41–52.
- Soares, A.A.M., 2010. Comment of 'Formation of chenier plain of the Doñana marshland (SW Spain): observations and geomorphic model' by A. Rodríguez Ramírez and C.M. Yáñez Camacho [Marine Geology 254, 187–196]. *Mar. Geol.* 275, 287–289.
- Soares, A.M.M., Martins, J.M.M., 2010. Radiocarbon dating of marine samples from Gulf of Cadiz: the reservoir effect. *Quat. Int.* 221, 9–12.
- Solares, J.M.M., Arroyo, A.L., 2004. The great historical 1755 earthquake. Effects and damage in Spain. *J. Seismol.* 8, 275–294.
- Szczucinski, W., Chaimanee, N., Niedzielski, P., Rachlewicz, G., Saisuttichai, D., Tepsuwam, T., Lorenc, S., Siepak, J., 2006. Environmental and geological impacts of the 26 December 2004 tsunami in coastal zone of Thailand—overview of short and long-term effects. *Pol. J. Environ. Stud.* 15, 793–810.
- Zazo, C., Goy, J.L., Somoza, L., Dabrio, C.J., Belluomini, G., Improta, S., Lario, J., Bardaji, T., Silva, P.G., 1994. Holocene sequence of sea-level fluctuations in relation to climatic trends in the Atlantic–Mediterranean linkage coast. *J. Coast. Res.* 10, 933–945.